ISSN: 1410-8917
e-ISSN: 2597-9914

Jurnal Kimia Sains dan Aplikasi 28 (2) (2025): 73-81

Jurnal Kimia Sains dan Aplikasi
Journal of Scientific and Applied Chemistry

Journal homepage: http://ejournal.undip.ac.id/index.php/ksa

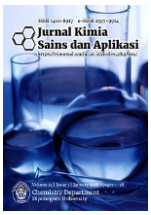

Performance Study of NiO-TiO_2-CuO Nanocomposite Supported by Reduced Graphene Oxide as an Anode Candidate for Lithium-Ion Battery Development

Muh Edihar [1,*], Kaharuddin Kaharuddin [1], Muhammad Nurdin [2,3], Maulidiyah Maulidiyah [2], Thamrin Azis [2], Mawaddah Zaqinah Diah [1]

[1] Department of Chemistry, Faculty of Science Technology and Health, Institut Sains Teknologi dan Kesehatan (ISTEK) 'Aisyiyah Kendari, Kendari, 93116, Southeast Sulawesi, Indonesia
[2] Department of Chemistry, Faculty of Mathematics and Natural Sciences, Universitas Halu Oleo, Kendari 93232, Southeast Sulawesi, Indonesia
[3] Nickel Research Institute, Universitas Muhammadiyah Kendari, Jl. K.H. Ahmad Dahlan No. 10 Kendari, Southeast Sulawesi, Indonesia

* Corresponding author: ediharmuh@gmail.com

https://doi.org/10.14710/jksa.28.2.73-81

Article Info

Article history:

Received: 29th September 2024
Revised: 04th February 2025
Accepted: 27th February 2025
Online: 28th February 2025

Keywords:
NiO-TiO_2-CuO/rGO; Reduced graphene oxide; Cyclic voltammetry; Electrochemistry; Specific capacity

Abstract

In an effort to enhance the performance of lithium-ion batteries (LIBs), this study developed a NiO-TiO_2-CuO nanocomposite supported by reduced graphene oxide (rGO) as an anode material. The nanocomposite was synthesized via a hydrothermal method and characterized using FTIR, XRD, and SEM-EDX techniques to understand its structure and material properties. The FTIR spectrum confirmed the presence of C=C bonds (1612-1512 cm^{-1}) and C–O bonds (1147-1099 cm^{-1}) from rGO, as well as Ni-O (408 cm^{-1}), Cu-O (669 cm^{-1}), and Ti- O (549 cm^{-1}). The XRD patterns revealed the crystalline phases of NiO at 2θ = 37° (111), 43° (200), and 62.8° (200); TiO_2 at 2θ = 25.3° (101), 48° (101), and 55° (211); and Cu-O at 2θ = 35.6° (111) and 39.8° (022). SEM-EDX images showed small aggregated particles forming a relatively uneven surface with spherical morphology, with an average particle size of 33.25 nm. Electrochemical testing using cyclic voltammetry (CV) demonstrated that the material exhibited a stable specific capacity (C_{sp}) of 6.3 mAh/g after five cycles at a scan rate of 1 V/s. Additionally, the specific capacity significantly increased to 44.15 mAh/g at a scan rate of 0.05 V/s, indicating excellent electrochemical performance. These results suggest that the NiO-TiO_2-CuO/rGO nanocomposite has potential as an efficient anode material for lithium-ion battery applications, offering good cycle stability and enhanced energy storage capacity.

1. Introduction

In the era of global energy transition, batteries have become a crucial component to support sustainable energy needs. Batteries require materials with high energy capacity and fast charge-discharge efficiency. Among the types of batteries currently being developed and widely applied in daily life, lithium-ion batteries (LIBs) stand out due to their capability as high-capacity energy storage devices, excellent cycle performance, and environmental friendliness. However, LIBs face challenges such as imbalance and relatively short battery lifespan [1]. To enhance battery performance and capacity, intensive research is being conducted to develop more advanced electrode materials. One promising approach is using transition metal oxide (TMO) composites. This combination offers the potential to improve energy storage capacity, optimize charge rates, and extend battery cycle life [2, 3, 4, 5, 6]. This research focuses on developing anode materials to improve capacity, cycle performance, and battery lifespan.

TMO materials such as NiO, CuO, and TiO_2 were selected for this study due to their extensively researched high capacities [7, 8]. NiO is recognized as a potential anode material because of its high theoretical capacity

and stable electrochemical properties. Even at low current densities, NiO demonstrates good reversible capacity and cycle stability [9]. Additionally, NiO exhibits high thermal stability, enabling it to withstand high-temperature and high-voltage battery operating conditions. Several studies have shown that NiO has sufficient ionic conductivity, making it an excellent conductive material for faster electron transfer [10, 11]. Another unique feature of NiO is its nanostructure, which allows it to be easily combined with other conductive materials. It has been reported that CuO coated with a thin conformal layer of NiO as an anode material exhibits excellent electrochemical performance. The presence of the NiO coating effectively facilitates ion diffusion into CuO, maintains the advantages of high surface area, and enhances cycle performance, leading to improved battery storage capacity [11].

In this study, TiO_2 was selected as a Ni-based electrode modification material based on literature reviews. Although progress has been made in the energy storage properties, capacity enhancement, and cycle stability of these materials, challenges remain for researchers. TiO_2 is considered a potential alternative anode material to replace commercially available graphite. Its advantages include preventing dendrite growth, low volume change, environmental friendliness, chemical stability, and low-cost [12, 13, 14, 15]. In electrochemical systems, TiO_2 holds significant promise for energy storage devices due to its fast electron transfer and reduced diffusion distance [15]. Furthermore, TiO_2 offers a high theoretical capacity (332 mAh g^{-1}) [16], but its low electronic conductivity limits its storage capacity. Therefore, developing TiO_2 with short diffusion lengths for electron and ion transport is essential. Various strategies have been explored to enhance TiO_2 capacity. Previous reports have shown that unique TiO_2@NiO structures deliver high capacity and cycle stability [17].

Conventional LIB anodes are typically composed of graphite. However, graphite can only operate at low potentials, limiting its theoretical capacity to meet the demands of modern electronics [18, 19]. To address this issue, we innovated by modifying graphite into reduced graphene oxide (rGO). Our investigation shows that rGO has a larger surface area than graphite [20], which can enhance battery capacity, cycling life, and charge-discharge efficiency [18]. Our studies also indicate that rGO combined with TiO_2 exhibits high energy storage and excellent electrochemical performance due to the well-organized three-phase composite electrode structure, ensuring stable electron transfer. This new structure reduces crystal expansion during the discharge process, enhances ion diffusion rates, and shortens electron transmission distances [18, 21].

Several previous studies have documented various comparisons involving different anode materials used in LIBs. These studies have examined various high-performance anodes and their electrochemical performance, with the findings compiled and presented in Table 1.

Based on our investigation, referring to Table 1 and several reviewed studies, the presence of TMO modifications has been shown to effectively enhance capacity, cycling life, and current stability. This research aims to evaluate the electrochemical performance of NiO-TiO_2-CuO nanocomposites supported by rGO as an energy storage electrode material for batteries. Material characterization using techniques such as XRD, SEM-EDX, and FTIR will be conducted to understand the structure and properties of the material. Additionally, electrochemical testing, including CV, will be used to assess the energy storage performance of the nanocomposite. Thus, this study is expected to contribute to developing more efficient and sustainable LIB materials.

2. Experimental

2.1. Materials

The materials used in this study were titanium dioxide (TiO_2) Degussa, ethanol deionized water, potassium permanganate ($KMnO_4$), hydrogen peroxide (H_2O_2), sulfuric acid (H_2SO_4), graphite, nickel sulfate hexahydrate ($NiSO_4.6H_2O$), sodium hydroxide (NaOH), copper sulfate pentahydrate ($CuSO_4.5H_2O$), sodium nitrate ($NaNO_3$), and potassium ferricyanide $K_3[Fe(CN)_6]$.

2.2. Synthesis of TiO_2

TiO_2 nanoparticles were prepared using the annealing method. Initially, 10 g of TiO_2 Degussa was dissolved in a mixture of deionized water and ethanol (1:1). The suspension was then sonicated for 1 hour at 80°C. After sonication, the suspension was filtered and dried at 500°C in a sealed container for 3 hours [22, 23, 24, 25].

Table 1. Research developments related to anodes

Material	C_{sp} (mAh/g)	Cycle	Reference
TiO_2	332	100	[16]
TiO_2/Ni/C nanohybrids	422	100	[26]
NiO/TiO_2	152.4	100	[27]
TiO_2/rGO (few-layers)	344.3	100	[28]
Ni-TiO_2/Graphene	283	200	[29]
TiO_2/NiO/rGO	245	200	[18]
NGr@NiO/TiO_2 hollow nanospheres	839.84	-	[30]
NiO-TiO_2-CuO/rGO nanocomposite	This research		

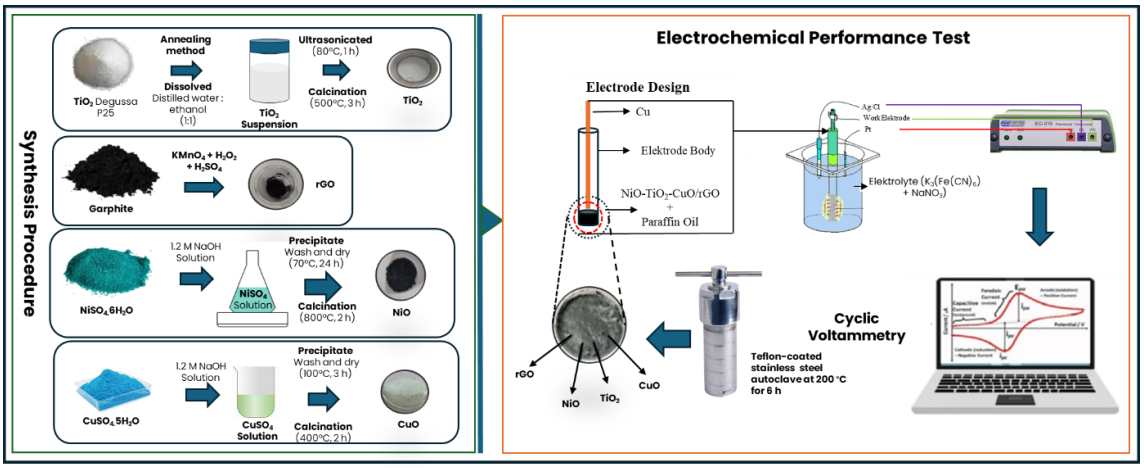

Figure 1. Research scheme of synthesis procedure for the NiO-TiO_2-CuO/rGO electrode

2.3. Synthesis of rGO

Graphene nanosheets incorporating rGO were synthesized using a modified Hummers' method [31, 32, 33]. Graphite powder, $KMnO_4$ (99%), H_2O_2 (30%), and H_2SO_4 (95%) were used. First, 25 mL of concentrated sulfuric acid was mixed with 1 g of graphite powder, and 3.5 g of $KMnO_4$ was slowly added to the solution. The mixture was stirred at 35°C for 2 hours, followed by the addition of 40 mL of deionized water. After 1 hour of stirring, hydrogen peroxide was added dropwise until the residual H_2O_2 gas disappeared. Graphene oxide was collected via centrifugation and dried at 70°C for 12 hours. The prepared graphene oxide was reduced using a solid-state microwave irradiation method. Briefly, graphene oxide powder (90 wt.%) was mixed with graphene nanosheet powder (10 wt.%), which acted as an effective microwave susceptor to produce high-quality rGO. The mixture was transferred to a quartz tube and reduced by microwave irradiation using a microwave oven. The microwave treatment was performed at 1600 W in pulsed irradiation mode [34].

2.4. Synthesis of NiO

NiO nanoparticles were synthesized using a precipitation method based on the literature [35, 36, 37]. A 250 mL solution of 1.2 M NaOH was slowly added dropwise into a 250 mL solution of 0.5 M $NiSO_4.6H_2O$ while stirring at 1000 rpm using a magnetic stirrer at room temperature. The resulting $Ni(OH)_2$ precipitate was separated and washed until free of sulfate ions, and the filtrate reached a neutral pH. The cleaned $Ni(OH)_2$ solid was dried in an oven at 70°C for 24 hours. The dried solid was then calcined at 800°C for 2 hours.

2.5. Synthesis of CuO

CuO nanoparticles were synthesized using a simple wet chemical method based on the literature [38, 39]. First, a 250 mL solution of 0.5 M $CuSO_4.5H_2O$ was prepared, and a 250 mL solution of 1.2 M NaOH was added dropwise using a burette while stirring at 1000 rpm with a magnetic stirrer at room temperature. The resulting $Cu(OH)_2$ precipitate was separated via filtration and washed with distilled water until free of sulfate ions, and the filtrate reached a neutral pH. The washed precipitate was dried in an oven at 100°C for 3 hours. The dried solid was then calcined at 400°C for 2 hours to obtain well-crystallized CuO nanoparticles.

2.6. Characterization

The electrode morphology was characterized using X-ray diffraction (XRD) (Shimadzu 6000) at $2\theta = 20–80°$ with Cu-Kα radiation ($\lambda = 1.54060$ Å). The nanocomposite morphology and atomic composition were analyzed using Scanning Electron Microscopy-Energy Dispersive X-ray spectroscopy (SEM-EDX) (HITACHI SU3500). Chemical bonds and functional groups were identified using Fourier Transform Infrared Spectroscopy (FT-IR) (Shimadzu Varian 4300 spectrophotometer). The electrochemical properties of the nanocomposite were characterized using cyclic voltammetry with a DY2100 potentiostat.

2.7. Preparation of NiO-TiO_2-CuO/rGO Electrode

The NiO-TiO_2-CuO/rGO composite was prepared with a mass ratio of NiO, TiO_2, CuO, and rGO at 10:30:10:50 (w/w%). The composite was dissolved in 50 mL of deionized water and sonicated for 1 hour. The suspension was then transferred to a 100 mL Teflon-lined stainless steel autoclave and heated at 200°C for 6 hours. After the reaction, the autoclave was cooled to room temperature, and the product was washed several times with deionized water and ethanol, followed by drying at 60°C for 24 hours. The product was further hydrothermally treated at 350°C for 2 hours. For electrode preparation, 0.05 g of the NiO-TiO_2-CuO/rGO nanocomposite was mixed with 0.3 g of paraffin oil and stirred at 400 rpm for 15 minutes while heating at 80°C. Finally, the NiO-TiO_2-CuO/rGO paste was packed into a 3 mm diameter glass tube, pressed gently, smoothed on the surface, and connected with a copper wire.

2.8. Electrochemical Performance Testing of NiO-TiO_2-CuO/rGO Electrode

The electrochemical properties of the NiO-TiO_2-CuO/rGO electrode were evaluated using cyclic voltammetry (CV) at scan rates of 1, 0.5, 0.2, 0.1, and 0.05 V/s within a potential range of -0.8 V to 0.8 V. The tests were conducted in an electrochemical cell containing 0.01 M $K_3[Fe(CN)_6]$ as the analyte and 0.1 M $NaNO_3$ as the electrolyte.

3. Results and Discussion

3.1. Morphological and Structure of NiO-TiO_2-CuO/rGO Nanocomposite

In this study, NiO-TiO_2-CuO/rGO was obtained by combining NiO, TiO_2, CuO, and rGO (Figure 1). The success of the research method was confirmed through various analytical techniques. FTIR analysis (Figure 2) and a literature review (Table 2) identify the functional groups corresponding to each spectral peak. Figure 2a shows a peak around 3400–3200 cm^{-1} (3219 cm^{-1}), indicating the presence of O-H stretching, which may originate from adsorbed water molecules on the nanocomposite surface [6] or oxygen-containing groups on the rGO surface. The peak around 2439–2312 cm^{-1} corresponds to C-H stretching, likely derived from organic solvents [40]. In this context, this band may indicate residual ethanol-based organic compounds during the TiO_2 synthesis process. Additionally, the peak at approximately 1147–1099 cm^{-1} corresponds to C-O stretching vibrations [41, 42], confirming the presence of oxygen in rGO or TMOs.

Figure 2b shows a small peak around 1612-1512 cm^{-1}, which can be attributed to the asymmetric stretching of C=C bonds in graphene sheet vibrations [43, 44]. The peaks around 669 cm^{-1} and 549 cm^{-1} are characteristic of the stretching vibrations of metal-oxygen bonds, specifically Cu-O and Ni-O [40, 45, 46]. The peak around 408 cm^{-1} is likely related to the stretching vibration of the Ti-O group in the nanocomposite structure [47].

The XRD pattern shows several intensity peaks that can be identified to determine the crystalline phases present in the nanocomposite. The XRD diffraction pattern of NiO-TiO_2-CuO/rGO is displayed in Figure 3. The dominant peaks observed between 2θ = 20° and 80° indicate the presence of various crystalline phases. Strong peaks around 2θ = 37°, 43°, and 62.8° were observed and can be indexed to the Miller indices (111), (200), and (220), which are characteristic of the NiO structure (ref. JCPDS 45-1049) [41, 42].

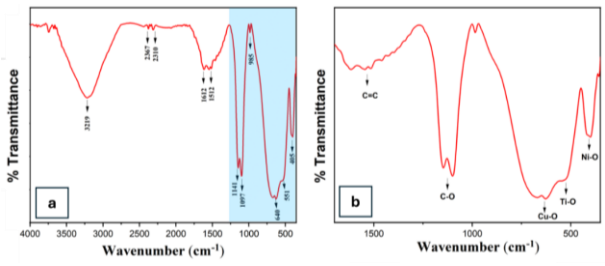

Figure 2. FTIR spectra of (a) NiO-TiO_2-CuO/rGO nanocomposite and (b) C=C, C-O, Ti-O, Cu-O and Ni-O

Table 2. Reference FTIR data for NiO-TiO_2-CuO/rGO

Functional groups	Reference wavenumber (cm^{-1})	Wavenumber (cm^{-1})	Reference
Ti-O	800-400	408	[45, 46]
Cu-O	601	669	[40]
Ni-O	549	550	[48]
C=C	1493–1630	1612-1512	[49]
C-O	1065-1226	1099	[49]

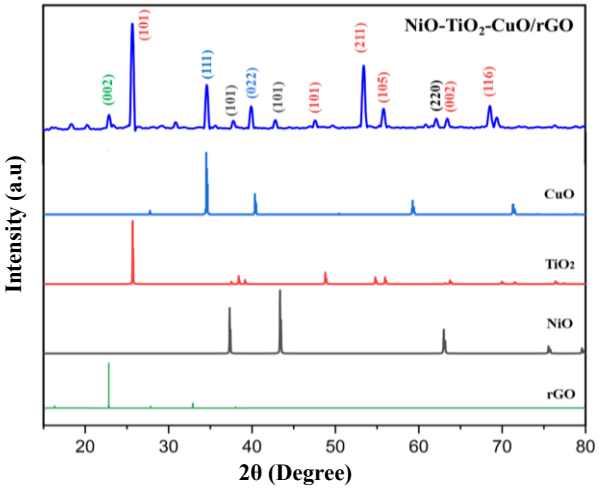

Figure 3. XRD pattern of NiO-TiO_2-CuO/rGO

Peaks observed around 2θ = 25.3°, 48°, and 55° were indexed to the Miller indices (101), (101), and (211), likely corresponding to TiO_2 in the anatase phase, which is commonly found in TiO_2 materials (ref. JCPDS 21-1272) [50]. Low-intensity peaks around 2θ = 35.6° and 39.8° were observed and can be indexed to the Miller indices (111) and (022), which may be associated with the CuO phase (ref. JCPDS 05-0661) [51]. A weak peak around 23.9° was observed and indexed to the Miller index (002), related to conjugated rGO [49]. Thus, the analyzed XRD diffraction pattern demonstrates the successful synthesis of NiO-TiO_2-CuO/rGO, and these findings are supported by EDX characterization data (Figure 4c).

To confirm the findings from the XRD analysis, SEM-EDX characterization was also conducted. Figure 4a provides a a thin-layer composite structure with well-dispersed nanocomposite particles. The observed structure shows small-sized particles aggregated together, forming a relatively uneven surface. Spherical nanoparticles appear to cover almost the entire layer surface, indicating good particle dispersion. Pore structures or small gaps are visible in some areas, supporting the porous nature of the material, as seen in Figure 4b. This is consistent with the morphology of the nanocomposite, where each component (NiO, TiO_2, CuO, and rGO) is integrated into a single structure [52, 53]. The NiO-TiO_2-CuO/rGO nanocomposite, subjected to high-temperature treatment, significantly influences particle size and minor changes in its structural shape.

The presence of each component (NiO, TiO_2, CuO, and rGO) in the material was further confirmed using EDX, as shown in Figure 4c. The results indicate the concentrations of NiO, TiO_2, CuO, and rGO to be 1.22%, 31.93%, 1.46%, and 4.12%, respectively. The inconsistent ratio likely results from non-homogeneous mixing, causing variations in composition across different regions. Since EDX analyzes specific points, it may not represent the overall material distribution. Additionally, during the heating process in the synthesis, some elements may have undergone segregation or changes in distribution. rGO may be more prone to burning or degradation than TiO_2 and CuO, which could explain its lower percentage in the EDX results than expected [54].

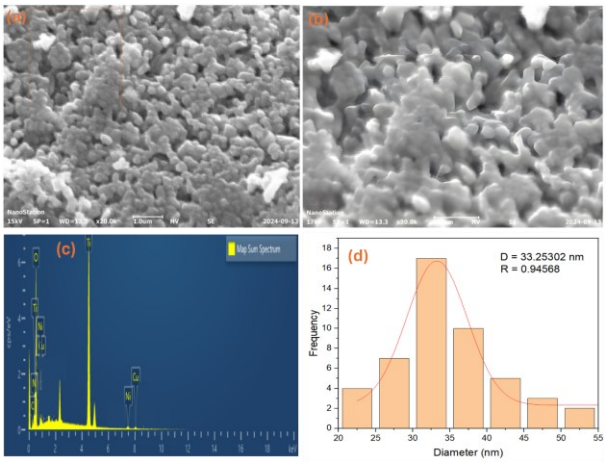

Figure 4. Morphology and composition of NiO-TiO_2-CuO/rGO: (a) 20,000× magnification, (b) 30,000× magnification, (c) Elemental composition, (d) Particle size distribution

To determine the particle size distribution of NiO-TiO_2-CuO/rGO, the SEM characterization results were processed using ImageJ software with its particle analysis feature. The particle diameter distribution ranges from 20 to 55 nm, with an average diameter of 33.25 nm and an R- squared value of 0.94568, indicating good data quality (Figure 4d). The consistency in particle size demonstrates that the synthesis method successfully produced a relatively uniform size distribution, confirming that the optimized material properties can enhance electrochemical performance.

3.2. Electrochemical Performace

The electrochemical performance of the NiO-TiO_2-CuO/rGO nanocomposite was tested using the CV (cyclic voltammetry) method. The testing was conducted using platinum as the counter electrode, Ag/AgCl as the reference electrode, and NiO-TiO_2-CuO/rGO as the working electrode. CV of the working electrode was performed at scan rates ranging from 5 to 100 mV/s within a voltage range of -0.8 to 0.8 V, as shown in Figures 5a and 5b.

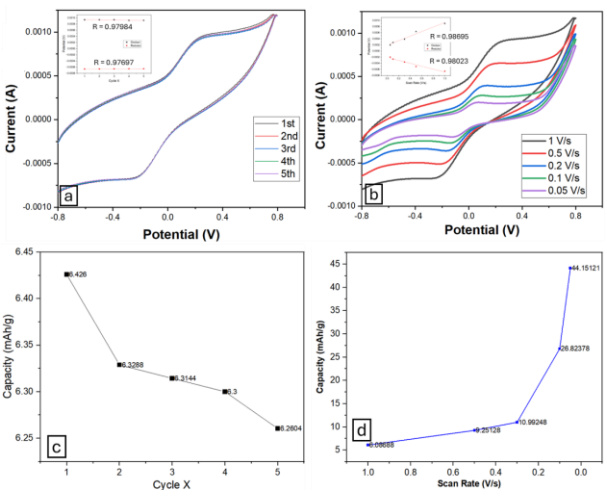

Figure 5. The voltammogram of NiO-TiO_2-CuO/rGO (a) first-five cycles at a scan rate of 1 V/s, (b) Cyclic variation, (c) C_{sp}: first-five cycles at a scan rate of 1 V/s, (d) C_{sp}: Cyclic variation

Determining anode stability requires multiple measurements. The formation of oxidation and reduction peaks and stable voltammograms allows for assessing anode reproducibility and reversibility. The curves in Figure 5a demonstrate the stable performance of the nanocomposite during the first to fifth CV cycles. This good stability is evidenced by the R values for the oxidation and reduction processes, which are 0.97984 and 0.97697, respectively, indicating high data quality. Minor changes in current intensity during the initial cycles suggest that the material undergoes an electrochemical activation process at the beginning of the cycles. This is a common phenomenon in the initial cycles, where the anode material adapts to store and release ions [55].

The curve in Figure 5b shows improved performance with each cycle, forming a well-defined voltammogram. The voltammogram indicates an increase in the area under the curve as the scan rate increases [56]. Each cycle exhibits a cathodic peak at ~0.18 V with an R-value of 0.98695 during discharge, followed by an anodic peak at ~-0.2 V with an R-value of 0.98023. R-values greater than 0.9 confirm the high quality of the data. This behavior suggests that the nanocomposite facilitates easier electron insertion and extraction processes, indicating that NiO-TiO_2-CuO/rGO has potential as an anode material with excellent electrochemical properties.

The graphs in Figures 5c and 5d show the capacity of NiO-TiO_2-CuO/rGO based on the voltammogram curves generated in Figures 5a and 5b. The calculation process follows Equation (1).

$$Q = \int_{V_1}^{V_2} I(V)dV \quad (1)$$

Plot the current (I) against the potential (V) and identify the relevant area under the curve (reduction or oxidation region). Then, integrate the current with respect to the potential to obtain the charge (Q). The specific capacity (C_{sp}) is then calculated using Equation (2).

$$C_{sp} = \frac{Q(C)}{3.6 \times m} \quad (2)$$

Where m is the mass (in grams), and the factor 3.6 converts Coulombs to milliampere-hours (mAh).

The curve in Figure 5c shows a decrease in C_{sp} for NiO-TiO_2-CuO/rGO over five cycles measured at a scan rate of 1 V/s, from 6.4 mAh/g in the first cycle to 6.3 mAh/g in the fifth cycle. This decline indicates that the electrode material experiences performance degradation as the number of cycles increases. We suspect the decrease in C_{sp} is due to electrode material degradation caused by forming a Solid Electrolyte Interphase (SEI) layer, consistent with previously documented reports [55, 57, 58]. From cycles 2 to 5, the specific capacity stabilizes at 6.3 mAh/g, suggesting that the electrode material begins to achieve cycle stability after the initial cycles.

The curve in Figure 5d shows an increase in C_{sp} (6.08, 9.25, 10.99, 26.82, and 44.15 mAh/g) for NiO-TiO_2-CuO/rGO as the scan rate decreases (1, 0.5, 0.2, 0.1, and 0.05 V/s). This phenomenon is commonly observed and

documented in previous studies [59]. In this study, a high scan rate (1 V/s) results in a lower C_{sp} (6.08 mAh/g) due to the shorter time available for ion intercalation processes. Conversely, a low scan rate (0.05 V/s) yields a higher C_{sp} (44.15 mAh/g) because it allows more time for electrochemical processes. In this case, the obtained capacity is relatively low, which may be attributed to slow reaction kinetics or hindered ion/charge transport within the material.

4. Conclusion

This study successfully developed a NiO-TiO_2-CuO/rGO nanocomposite as an anode material for lithium-ion batteries. Characterization results demonstrate that the material possesses a well-defined crystalline structure with homogeneous particle distribution and an average particle size of 33.25 nm. Electrochemical testing using CV revealed that the nanocomposite exhibits a stable C_{sp} of 6.3 mAh/g after five cycles at a scan rate of 1 V/s, as well as an increased specific capacity of up to 44.15 mAh/g at a scan rate of 0.05 V/s. This enhanced electrochemical performance is attributed to its high cycle stability and improved energy storage capability. Therefore, the NiO-TiO_2-CuO/rGO nanocomposite shows great potential as an efficient and sustainable anode material for lithium-ion battery applications, contributing to the advancement of future energy storage technologies.

Acknowledgments

We acknowledge the financial support from the Ministry of Education, Culture, Research and Technology of the Republic of Indonesia under the Beginner Lecturer Research (PDP) award grant no. 111/E5/PG.02.00.PL/2024 and 576/LL9/PK.00.PG/2024, 04/K/LPPM/ISTEK-AK/VI/2024.

References

[1] Lukas Mauler, Fabian Duffner, Wolfgang G. Zeier, Jens Leker, Battery cost forecasting: a review of methods and results with an outlook to 2050, *Energy & Environmental Science*, 14, 9, (2021), 4712-4739 https://doi.org/10.1039/D1EE01530C

[2] Huili Shi, Chaoyun Shi, Zhitong Jia, Long Zhang, Haifeng Wang, Jingbo Chen, Titanium dioxide-based anode materials for lithium-ion batteries: structure and synthesis, *RSC Advances*, 12, 52, (2022), 33641-33652 https://doi.org/10.1039/D2RA05442F

[3] Mingbo Zheng, Hao Tang, Lulu Li, Qin Hu, Li Zhang, Huaiguo Xue, Huan Pang, Hierarchically Nanostructured Transition Metal Oxides for Lithium-Ion Batteries, *Advanced Science*, 5, 3, (2018), 1700592 https://doi.org/10.1002/advs.201700592

[4] Yongchao Huang, Hao Yang, Tuzhi Xiong, David Adekoya, Weitao Qiu, Zhongmin Wang, Shanqing Zhang, M. Sadeeq Balogun, Adsorption energy engineering of nickel oxide hybrid nanosheets for high areal capacity flexible lithium-ion batteries, *Energy Storage Materials*, 25, (2020), 41-51 https://doi.org/10.1016/j.ensm.2019.11.001

[5] Chunxiao Lv, Xianfeng Yang, Ahmad Umar, Yanzhi Xia, Yi Jia, Lu Shang, Tierui Zhang, Dongjiang Yang, Architecture-controlled synthesis of M_xO_y (M = Ni, Fe, Cu) microfibres from seaweed biomass for high-performance lithium ion battery anodes, *Journal of Materials Chemistry A*, 3, 45, (2015), 22708-22715 https://doi.org/10.1039/C5TA06393K

[6] Bakht Mand Khan, Won Chun Oh, Prawit Nuengmatch, Kefayat Ullah, Role of graphene-based nanocomposites as anode material for Lithium-ion batteries, *Materials Science and Engineering: B*, 287, (2023), 116141 https://doi.org/10.1016/j.mseb.2022.116141

[7] Wenxing Liu, Tianhao Yao, Sanmu Xie, Yiyi She, Hongkang Wang, Integrating TiO_2/SiO_2 into Electrospun Carbon Nanofibers towards Superior Lithium Storage Performance, *Nanomaterials*, 9, 1, (2019), 68 https://doi.org/10.3390/nano9010068

[8] Xiaoyu Dong, Xing Zheng, Yichen Deng, Lingfeng Wang, Haiping Hong, Zhicheng Ju, SiO_2/N-doped graphene aerogel composite anode for lithium-ion batteries, *Journal of Materials Science*, 55, 27, (2020), 13023-13035 https://doi.org/10.1007/s10853-020-04905-y

[9] Junke Ou, Shugen Wu, Lin Yang, Hao Wang, Facile Preparation of NiO@graphene Nanocomposite with Superior Performances as Anode for Li-ion Batteries, *Acta Metallurgica Sinica (English Letters)*, 35, 2, (2022), 212-222 https://doi.org/10.1007/s40195-021-01283-5

[10] Song Liu, Hongying Hou, Xianxi Liu, Jixiang Duan, Yuan Yao, Qishu Liao, High-performance hierarchical cypress-like CuO/Cu_2O/Cu anode for lithium ion battery, *Ionics*, 23, 5, (2017), 1075-1082 https://doi.org/10.1007/s11581-016-1933-5

[11] Xun Sun, Zhe Wang, Xinping Ai, Jinping Zhou, CuO nanosheets embedded on carbon microspheres as high-performance anode material in lithium-ion batteries, *Science China Materials*, 66, 8, (2023), 3026-3038 https://doi.org/10.1007/s40843-023-2452-4

[12] M. Mancini, F. Nobili, R. Tossici, M. Wohlfahrt-Mehrens, R. Marassi, High performance, environmentally friendly and low cost anodes for lithium-ion battery based on TiO_2 anatase and water soluble binder carboxymethyl cellulose, *Journal of Power Sources*, 196, 22, (2011), 9665-9671 https://doi.org/10.1016/j.jpowsour.2011.07.028

[13] Yue Wang, Suqin Liu, Kelong Huang, Dong Fang, Shuxin Zhuang, Electrochemical properties of freestanding TiO_2 nanotube membranes annealed in Ar for lithium anode material, *Journal of Solid State Electrochemistry*, 16, 2, (2012), 723-729 https://doi.org/10.1007/s10008-011-1417-5

[14] Zhen Wei, Zheng Liu, Rongrong Jiang, Chaoqing Bian, Tao Huang, Aishui Yu, TiO_2 nanotube array film prepared by anodization as anode material for lithium ion batteries, *Journal of Solid State Electrochemistry*, 14, 6, (2010), 1045-1050 https://doi.org/10.1007/s10008-009-0910-6

[15] Tamilselvan Appadurai, Chandrasekar M. Subramaniyam, Rajesh Kuppusamy, Smagul Karazhanov, Balakumar Subramanian, Electrochemical Performance of Nitrogen-Doped TiO_2 Nanotubes as Electrode Material for

Supercapacitor and Li-Ion Battery, *Molecules*, 24, 16, (2019), 2952 https://doi.org/10.3390/molecules24162952

[16] Zhenguo Yang, Daiwon Choi, Sebastien Kerisit, Kevin M. Rosso, Donghai Wang, Jason Zhang, Gordon Graff, Jun Liu, Nanostructures and lithium electrochemical reactivity of lithium titanites and titanium oxides: A review, *Journal of Power Sources*, 192, 2, (2009), 588-598 https://doi.org/10.1016/j.jpowsour.2009.02.038

[17] Guojian Li, Hao Hu, Qiancheng Zhu, Ying Yu, Interconnected mesoporous NiO sheets deposited onto TiO_2 nanosheet arrays as binder-free anode materials with enhanced performance for lithium ion batteries, *RSC Advances*, 5, 122, (2015), 101247-101256 https://doi.org/10.1039/C5RA16894E

[18] Zehua Chen, Yu Gao, Qixiang Zhang, Liangliang Li, Pengcheng Ma, Baolin Xing, Jianliang Cao, Guang Sun, Hari Bala, Chuanxiang Zhang, Zhanying Zhang, Yanyang zeng, TiO_2/NiO/reduced graphene oxide nanocomposites as anode materials for high-performance lithium ion batteries, *Journal of Alloys and Compounds*, 774, (2019), 873-878 https://doi.org/10.1016/j.jallcom.2018.10.010

[19] Tereza M. Paronyan, Arjun Kumar Thapa, Andriy Sherehiy, Jacek B. Jasinski, John Samuel Dilip Jangam, Incommensurate Graphene Foam as a High Capacity Lithium Intercalation Anode, *Scientific Reports*, 7, (2017), 39944 https://doi.org/10.1038/srep39944

[20] Hassan Abbas Alshamsi, Sura K. Ali, Salam H. Alwan Altaa, Green Synthesis and Characterization of Reduced Graphene Oxide (RGO) using *Sabdarriffa* L extract and its Solubility Property, *Journal of Physics: Conference Series*, 1664, (2020), 012058 https://doi.org/10.1088/1742-6596/1664/1/012058

[21] Hong-En Wang, Xu Zhao, Xuecheng Li, Zhenyu Wang, Chaofeng Liu, Zhouguang Lu, Wenjun Zhang, Guozhong Cao, rGO/SnS_2/TiO_2 heterostructured composite with dual-confinement for enhanced lithium-ion storage, *Journal of Materials Chemistry A*, 5, 47, (2017), 25056-25063 https://doi.org/10.1039/C7TA08616D

[22] La Ode Agus Salim, Muhammad Zakir Muzakkar, Ahmad Zaeni, Maulidiyah Maulidiyah, Muhammad Nurdin, Siti Naqiyah Sadikin, Jaenuddin Ridwan, Akrajas Ali Umar, Improved photoactivity of TiO_2 photoanode of dye-sensitized solar cells by sulfur doping, *Journal of Physics and Chemistry of Solids*, 175, (2023), 111224 https://doi.org/10.1016/j.jpcs.2023.111224

[23] Manmohan Lal, Praveen Sharma, Chhotu Ram, Synthesis and photocatalytic potential of Nd-doped TiO_2 under UV and solar light irradiation using a sol-gel ultrasonication method, *Results in Materials*, 15, (2022), 100308 https://doi.org/10.1016/j.rinma.2022.100308

[24] Nasriadi Dali, Alfina Amelia Amasi, Irwan Irwan, Faizal Mustapa, Maulidiyah Maulidiyah, Muhammad Nurdin, Highly sensitive determination of Pb (II) ions using graphene paste electrode modified TiO_2-ionophore calix[6]arene composite, *AIP Conference Proceedings*, 2719, 1, (2023), 030015 https://doi.org/10.1063/5.0133282

[25] Zul Arham, Annisa Zalfa Al Ikhwan, Muhammad Edihar, Abdul Haris Watoni, Irwan Irwan, Muhammad Nurdin, Maulidiyah Maulidiyah, Green Pesticide High Activity Based on TiO_2 Nanosuspension Incorporated Silver Microspheres Against *Phytophthora palmivora*, *Indian Journal of Microbiology*, 64, 4, (2024), 1826-1834 https://doi.org/10.1007/s12088-024-01239-0

[26] Xiaoyan Wang, Dong Zhao, Chao Wang, Yonggao Xia, Wenshuai Jiang, Senlin Xia, Shanshan Yin, Xiuxia Zuo, Ezzeldin Metwalli, Ying Xiao, Zaicheng Sun, Jin Zhu, Peter Müller-Buschbaum, Ya-Jun Cheng, Role of Nickel Nanoparticles in High-Performance TiO_2/Ni/Carbon Nanohybrid Lithium/Sodium-Ion Battery Anodes, *Chemistry – An Asian Journal*, 14, 9, (2019), 1557-1569 https://doi.org/10.1002/asia.201900231

[27] Hong Zhang, Binqiang Tian, Jian Xue, Guoqing Ding, Xiaoming Ji, Yang Cao, Hierarchical non-woven fabric NiO/TiO_2 film as an efficient anode material for lithium-ion batteries, *RSC Advances*, 9, 43, (2019), 24682-24687 https://doi.org/10.1039/C9RA04947A

[28] Chun-Yan Geng, Jin Yu, Fa-Nian Shi, Few-layers of graphene modified TiO_2/graphene composites with excellent electrochemical properties for lithium-ion battery, *Ionics*, 25, 7, (2019), 3059-3068 https://doi.org/10.1007/s11581-019-02894-w

[29] Gang Wang, Qian Zhang, Kai Zhang, Bo Gu, Lin Cheng, Qiaojun Nie, Ming Zhang, Zhongrong Shen, Designing High-mass Loading 2D Ni-TiO_2/graphene Pellet Electrodes for Lithium Metal Batteries, *ChemistrySelect*, 8, 21, (2023), e202300961 https://doi.org/10.1002/slct.202300961

[30] Thamrin Azis, Lintan Ashari, Muhammad Zakir Muzakkar, Muhammad Nurdin, La Ode Muhammad Zuhdi Mulkiyan, La Ode Agus Salim, Muh Edihar, Akrajas Ali Umar, Enhancing cyclic voltammetry performance with N-graphene -supported coupled NiO/TiO_2 hollow nanospheres as superior anode material, *Chemical Papers*, 78, 8, (2024), 4719-4731 https://doi.org/10.1007/s11696-024-03408-3

[31] Muhammad Helmi Abdul Kudus, Muhammad Razlan Zakaria, Hazizan Md Akil, Faheem Ullah, Fatima Javed, Oxidation of graphene via a simplified Hummers' method for graphene-diamine colloid production, *Journal of King Saud University - Science*, 32, 1, (2020), 910-913 https://doi.org/10.1016/j.jksus.2019.05.002

[32] K. Narasimharao, G. Venkata Ramana, D. Sreedhar, V. Vasudevarao, Synthesis of graphene oxide by modified hummers method and hydrothermal synthesis of graphene-NiO nano composite for supercapacitor application, *Journal of Material Sciences & Engineering*, 5, 6, (2016), 1000284

[33] Ji Chen, Bowen Yao, Chun Li, Gaoquan Shi, An improved Hummers method for eco-friendly synthesis of graphene oxide, *Carbon*, 64, (2013), 225-229 https://doi.org/10.1016/j.carbon.2013.07.055

[34] Ghulam Ali, Asad Mehmood, Heung Yong Ha, Jaehoon Kim, Kyung Yoon Chung, Reduced graphene oxide as a stable and high-capacity cathode material for Na-ion batteries, *Scientific Reports*, 7, 1, (2017), 40910 https://doi.org/10.1038/srep40910

[35] Mahendra Singh Yadav, S. K. Tripathi, Synthesis and characterization of nanocomposite NiO/activated charcoal electrodes for supercapacitor application, *Ionics*, 23, 10, (2017), 2919-2930 https://doi.org/10.1007/s11581-017-2026-9

[36] Umesh P. Gawai, Shilpa D. Kamble, Sanjay K. Gurav, Manvendra N. Singh, Ashok K. Yadav, Shambhu N. Jha, Niranjan P. Lalla, Milind R. Bodke, Mahendra D. Shirsat, Babasaheb N. Dole, Microwave-Assisted Coprecipitation Synthesis and Local Structural Investigation on NiO, β -$Ni(OH)_2/Co_3O_4$ Nanosheets, and Co_3O_4 Nanorods Using X-ray Absorption Spectroscopy at Co – Ni K-edge and Synchrotron X-ray Diffraction, *ACS Omega*, 7, 8, (2022), 6700-6709 https://doi.org/10.1021/acsomega.1c06179

[37] Anadi Krishna Atul, Sunil Kumar Srivastava, Ajai Kumar Gupta, Neelabh Srivastava, Synthesis and Characterization of NiO Nanoparticles by Chemical Co-precipitation Method: an Easy and Cost-Effective Approach, *Brazilian Journal of Physics*, 52, 1, (2021), 2 https://doi.org/10.1007/s13538-021-01006-2

[38] Anita Sagadevan Ethiraj, Dae Joon Kang, Synthesis and characterization of CuO nanowires by a simple wet chemical method, *Nanoscale Research Letters*, 7, 1, (2012), 70 https://doi.org/10.1186/1556-276X-7-70

[39] Thi Ha Tran, Viet Tuyen Nguyen, Copper Oxide Nanomaterials Prepared by Solution Methods, Some Properties, and Potential Applications: A Brief Review, *International Scholarly Research Notices*, 2014, 1, (2014), 856592 https://doi.org/10.1155/2014/856592

[40] Alina Matei, Gabriel Craciun, Cosmin Romanitan, Cristina Pachiu, Vasilica Tucureanu, Biosynthesis and Characterization of Copper Oxide Nanoparticles, *Engineering Proceedings*, 37, 1, (2023), 54 https://doi.org/10.3390/ECP2023-14629

[41] Yu-Feng Sun, Wang Jian, Pei-Hua Li, Meng Yang, Xing-Jiu Huang, Highly sensitive electrochemical detection of Pb(II) based on excellent adsorption and surface Ni(II)/Ni(III) cycle of porous flower-like NiO/rGO nanocomposite, *Sensors and Actuators B: Chemical*, 292, (2019), 136-147 https://doi.org/10.1016/j.snb.2019.04.131

[42] Marilena Carbone, Elvira Maria Bauer, Laura Micheli, Mauro Missori, NiO morphology dependent optical and electrochemical properties, *Colloids and Surfaces A: Physicochemical and Engineering Aspects*, 532, (2017), 178-182 https://doi.org/10.1016/j.colsurfa.2017.05.046

[43] Kamal Batra, Sasmita Nayak, Sanjay K. Behura, Omkar Jani, Optimizing Performance Parameters of Chemically-Derived Graphene/p-Si Heterojunction Solar Cell, *Journal of Nanoscience and Nanotechnology*, 15, 7, (2015), 4877-4882 https://doi.org/10.1166/jnn.2015.9818

[44] Pietro Steiner, Nanoscopic infrared characterisation of graphene oxide, University of Manchester Manchester, UK, 2018

[45] M. Sathish, B. Viswanathan, R. P. Viswanath, Chinnakonda S. Gopinath, Synthesis, Characterization, Electronic Structure, and Photocatalytic Activity of Nitrogen-Doped TiO_2 Nanocatalyst, *Chemistry of Materials*, 17, 25, (2005), 6349-6353 https://doi.org/10.1021/cm052047v

[46] Xili Lu, Xiuqian Lv, Zhijie Sun, Yufeng Zheng, Nanocomposites of poly(L-lactide) and surface-grafted TiO_2 nanoparticles: Synthesis and characterization, *European Polymer Journal*, 44, 8, (2008), 2476-2481 https://doi.org/10.1016/j.eurpolymj.2008.06.002

[47] L. S. Chougala, M. S. Yatnatti, R. K. Linganagoudar, R. R. Kamble, J. S. Kadadevarmath, A simple approach on synthesis of TiO_2 nanoparticles and its application in dye sensitized solar cells, *Journal of Nano- and Electronic Physics*, 9, 4, (2017), 04005

[48] Sung-Jei Hong, Hyuk-Jun Mun, Byeong-Jun Kim, Young-Sung Kim, Characterization of Nickel Oxide Nanoparticles Synthesized under Low Temperature, *Micromachines*, 12, 10, (2021), 1168 https://doi.org/10.3390/mi12101168

[49] Prateek Viprya, Dhruva Kumar, Suhas Kowshik, Study of Different Properties of Graphene Oxide (GO) and Reduced Graphene Oxide (rGO), *Engineering Proceedings*, 59, 1, (2023), 84 https://doi.org/10.3390/engproc2023059084

[50] M. M. El-Desoky, Ibrahim Morad, M. H. Wasfy, A. F. Mansour, Synthesis, structural and electrical properties of PVA/TiO_2 nanocomposite films with different TiO_2 phases prepared by sol–gel technique, *Journal of Materials Science: Materials in Electronics*, 31, 20, (2020), 17574-17584 https://doi.org/10.1007/s10854-020-04313-7

[51] Zhe Li, Qinghua Yan, Qian Jiang, Yanshan Gao, Tianshan Xue, Renna Li, Yuefeng Liu, Qiang Wang, Oxygen vacancy mediated $Cu_yCo_{3-y}Fe_1O_x$ mixed oxide as highly active and stable toluene oxidation catalyst by multiple phase interfaces formation and metal doping effect, *Applied Catalysis B: Environmental*, 269, (2020), 118827 https://doi.org/10.1016/j.apcatb.2020.118827

[52] Harini S., Anto Feradrick Samson V., Victor Antony Raj M., Madhavan J., Fabrication of NiO/TiO_2/rGO nanocomposites as a quasi-solid-state asymmetric supercapacitor: Paving the way for PhotoSupercapacitor application, *Materials Today Sustainability*, 28, (2024), 100972 https://doi.org/10.1016/j.mtsust.2024.100972

[53] R. Rameshbabu, Niraj Kumar, Gina Pecchi, Eduardo J. Delgado, C. Karthikeyan, R. V. Mangalaraja, Ultrasound-assisted synthesis of rGO supported NiO-TiO_2 nanocomposite: An efficient superior sonophotocatalyst under diffused sunlight, *Journal of Environmental Chemical Engineering*, 10, 3, (2022), 107701 https://doi.org/10.1016/j.jece.2022.107701

[54] Jelena D. Jovanovic, Stevan N. Blagojevic, Borivoj K. Adnadjevic, The Effects of rGO Content and Drying Method on the Textural, Mechanical, and Thermal Properties of rGO/Polymer Composites, *Polymers*, 15, 5, (2023), 1287 https://doi.org/10.3390/polym15051287

[55] Jürgen Janek, Wolfgang G. Zeier, A solid future for battery development, *Nature Energy*, 1, 9, (2016), 16141 https://doi.org/10.1038/nenergy.2016.141

[56] A. W. P. Fung, Z. H. Wang, K. Lu, M. S. Dresselhaus, R. W. Pekala, Characterization of carbon aerogels by transport measurements, *Journal of Materials*

Research, 8, 8, (1993), 1875-1885
https://doi.org/10.1557/JMR.1993.1875

[57] Taehoon Kim, Luis K. Ono, Nicole Fleck, Sonia R. Raga, Yabing Qi, Transition metal speciation as a degradation mechanism with the formation of a solid-electrolyte interphase (SEI) in Ni-rich transition metal oxide cathodes, *Journal of Materials Chemistry A*, 6, 29, (2018), 14449-14463
https://doi.org/10.1039/C8TA02622J

[58] Changjun Zhang, Deconvoluting degradation mechanisms, *Nature Energy*, 9, 9, (2024), 1051-1051
https://doi.org/10.1038/s41560-024-01646-z

[59] Dong Yan, Caiyan Yu, Xiaojie Zhang, Jiabao Li, Junfeng Li, Ting Lu, Likun Pan, Enhanced electrochemical performances of anatase TiO_2 nanotubes by synergetic doping of Ni and N for sodium-ion batteries, *Electrochimica Acta*, 254, (2017), 130-139
https://doi.org/10.1016/j.electacta.2017.09.120